Where to go green and who benefits? Coordinated green infrastructure planning for cross-regional flood risk management

Hong, Qichen; Zhang, Haoxun; Chen, Bin; Nijhuis, Steffen; Xie, Yuting

DOI
10.1016/j.ijdrr.2025.105856

Publication date
2025

Document Version
Final published version

Published in
International Journal of Disaster Risk Reduction

International Journal of Disaster Risk Reduction 130 (2025) 105856

Contents lists available at ScienceDirect

International Journal of Disaster Risk Reduction

journal homepage: www.elsevier.com/locate/ijdrr

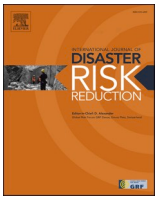

Where to go green and who benefits? Coordinated green infrastructure planning for cross-regional flood risk management

Qichen Hong [a], Haoxun Zhang [a], Bin Chen [a,b], Steffen Nijhuis [c], Yuting Xie [a,*]

[a] Institute of Landscape Architecture, College of Agriculture and Biotechnology, Zhejiang University, Hangzhou, 310058, China
[b] Hanjia Design Group Co. Ltd, Hangzhou, 310005, China
[c] Department of Urbanism, Faculty of Architecture and the Built Environment, Delft University of Technology, Delft, 2628 BL, the Netherlands

ARTICLE INFO

Keywords:
Flood risk management
Green infrastructure
Cross-regional planning
Nature-based solutions
Watershed heterogeneity

ABSTRACT

Global climate change and rapid urbanization have intensified flood risks worldwide, especially in cross-regional watersheds where jurisdictions often implement mitigation strategies independently. Although grey infrastructure is widely used to address these heightened risks, its fragmented application frequently shifts hazards to adjacent regions and causes adverse ecological impacts. In contrast, green infrastructure (GI), an interconnected network of natural and semi-natural areas, offers a promising nature-based solution, yet variability in terrain, soils, land use, and hydrological connectivity complicates the development of universal GI planning guidelines. Thus, this study addresses two critical questions: (1) How do changes in flood risk management performance (FRMP) in one region affect neighboring regions? (2) How can GI planning be tailored to watershed heterogeneity? Focusing on three contiguous regions in China's Yangtze River Delta Ecological Green Integration Demonstration Zone, we simulated flood processes using the SCS-MIKE11 hydrological-hydrodynamic model, optimized GI spatial configurations via Simulated Annealing, and applied the TOPSIS to select configurations that balance FRMP across all regions. Results show: (1) significant interregional FRMP correlations, with midstream negatively correlated with upstream (p <0.001) and downstream (p <0.001); (2) dispersed GI spatial configurations better accommodate watershed heterogeneity; (3) prioritizing FRMP at regional boundaries when configuring GI effectively mitigates watershed-wide flood risks; (4) distributive justice, integrated land and water management are essential for cross-regional flood challenges. This study reveals interregional FRMP coupling and pioneers a heterogeneity-responsive GI optimization, offering planners a novel decision-support tool for coordinated GI planning for cross-regional flood risk management.

1. Introduction

In recent years, global climate change and rapid urbanization have increased the frequency and intensity of floods [1–3], posing severe threats to human safety and property [4,5]. These risks are particularly acute in cross-regional watersheds, especially transboundary watersheds where lives over 2.8 billion people (approximately 42 % of the world population) and produce around 22,000 km^3 river discharge every year (more than 50 % of the global river discharge) [6]. Given the inherent connectivity of rivers, jurisdictions within the same watershed share common riverine fates [7]. Fragmented flood risk management strategies, where individual

* Corresponding author. 866 Yuhangtang Road, China.
E-mail address: xieyuting@zju.edu.cn (Y. Xie).

https://doi.org/10.1016/j.ijdrr.2025.105856
Received 14 May 2025; Received in revised form 3 September 2025; Accepted 5 October 2025
Available online 6 October 2025

jurisdictions addresses floods in isolation, often overlook the impact on others and may exacerbate conflicts between regions [8,9]. Consequently, flood risk management has evolved into a complex challenge that demands cross-regional coordination.

However, coordination of flood risk management across regions remains insufficient: over 20 countries lack formal coordination mechanisms, and only eight have enhanced transboundary cooperation between 2020 and 2023 [10]. Flood risk management therefore continues to rely on conventional grey infrastructure—including dams, dikes, and drainage networks—to rapidly collect and convey runoff for localized protection [11–13]. However, these isolated strategies frequently exacerbate hazards in neighboring regions and fail to reduce overall watershed-level flood risk [14,15]. For instance, hydraulic simulations in the Vietnamese Mekong River Basin revealed that upstream high-dike construction increased downstream peak water level by 9–13 cm during the 2011 flood event [16]. Similarly, research in the Susquehanna River Basin demonstrated that regions outside dike protection experienced approximately 25 % expansion in 100-year flood inundation extent, with some downstream regions facing flood depth increases up to 2 m [17]. While these case studies have quantified specific impacts of flood interventions across regions, they represent isolated analyses limited to specific events and local contexts. What remains lacking is a generalizable framework for predicting interregional flood risk relationships across varied watershed conditions. Clearly established interregional flood risk relationships remain absent, hindering evidence-based negotiations among stakeholders of different regions [8]. This limited transferability of existing knowledge makes it difficult to develop coordinated strategies that balance regional benefits in diverse watershed systems. Consequently, to inform transferable, evidence-based coordination strategies, this study raises a critical research question: How do changes in flood risk management performance (FRMP) in one region affect neighboring regions?

Beyond transferring flood risks, grey infrastructure strategies also generate substantial ecological impacts, including sediment starvation, water quality degradation and biodiversity loss, with upstream interventions particularly affecting downstream regions [18–21]. Research in the Volta River watershed demonstrated that the construction of the Akosombo dam reduced sediment flux to downstream regions by over 90 % [20], diminishing nutrients and degrading water quality [22]. Similarly, dikes disrupt the exchange of water, sediment and organisms between river and floodplain, substantially reducing biodiversity and ecosystem productivity in downstream regions [22]. These ecological consequences underscore both the urgent need for nature-based flood risk management solutions and the challenges of coordinating interventions across regions [23,24].

Nature-based solutions—especially green infrastructure (GI)—offer distinct advantages in addressing flood risk transfer and ecosystem degradation. GI refers to a strategically planned network of natural and semi-natural spaces (such as wetlands and woodlands) that utilizes natural processes to manage flood risk while providing broader ecosystem services [25–30]. As an interconnected network, GI can attenuate flood peaks beyond jurisdictional borders, enhance water quality, and sustain habitat connectivity at the watershed scale [31,32]. Empirical evidence underscores these effects: in Milan's urban watersheds, a 25 % expansion of GI halved flood-related damages and reduced the flood-exposed population by 40 % [33]. Beyond flood attenuation, GI enhances pollutant filtration [11,34] and provides continuous habitats that bolster biodiversity across the watershed [35]. Accordingly, integrating multi-functional GI with conventional grey infrastructure has risen to prominence as a sustainable, coordinated strategy for cross-regional flood risk management [26,27,36].

However, realizing GI's full potential requires spatial planning that explicitly accounts for watershed heterogeneity—variations in terrain, soils, land use, and hydrological connectivity—which precludes universal GI planning guidelines [37,38]. Context-specific studies have thus far yielded divergent recommendations. For watersheds with significant terrain variation, GI is recommended to place along river corridors to regulate runoff [39–41], whereas in flat watersheds, downstream areas are considered more suitable for GI placement to maximize infiltration [42]. Furthermore, when soil texture and land-use distributions are taken into account, a dispersed GI configuration outperforms clustered layouts with respect to flood risk mitigation efficacy [1]. Collectively, these findings highlight the critical influence of watershed heterogeneity on GI's FRMP. This raises another critical research question: How can GI spatial configuration optimization effectively respond to watershed heterogeneity?

Therefore, to address these two critical research questions, this study develops a decision-making framework for coordinated GI planning that explicitly accounts for both interregional flood risk interactions and watershed heterogeneity. We focus on China's Yangtze River Delta Ecological Green Integration Demonstration Zone, spanning three administrative regions: Qingpu (Shanghai), Wujiang (Jiangsu), and Jiashan (Zhejiang). In this zone, extensive polder systems—diked lowlands equipped with sluices and pumps—have significantly altered hydrological connectivity [43–45], increasing local drainage capacity within diked areas but also exacerbating flood risks and intensifying flood management conflicts among neighboring regions [46–48].

To fill this gap, we first applied correlation analysis to outputs from the SCS–MIKE11 hydrological–hydrodynamic model to quantify how FRMP improvements in one region influence neighboring regions, revealing that uncoordinated interventions can undermine benefits elsewhere and underscoring the need for interregional coordination. Next, we tailor GI spatial configurations to watershed heterogeneity—using the Simulated Annealing algorithm (SA) for optimization and the Technique for Order of Preference by Similarity to Ideal Solution (TOPSIS) for multi-criteria decision analysis—and demonstrate that dispersed, boundary-focused configurations balance FRMP more effectively than uncoordinated or uniform allocations. Finally, we synthesize these insights into a replicable decision-making framework to guide planners in implementing adaptive and coordinated GI planning for flood risk management across heterogeneous watersheds.

2. Methods

As illustrated in Fig. 1, the decision-making framework for coordinated GI planning for cross-regional flood risk management in this study involves four interconnected steps. The process begins by generating random GI spatial configurations through modifications to land use and land cover (LULC), adhering to area constraints defined by local territorial planning. These configurations are evaluated

using the SCS-MIKE11 hydrological-hydrodynamic coupled model, with peak water level reductions at nine monitoring stations, representing FRMP across three regions, set as the optimization objectives. Next, the SA is applied to determine optimal GI spatial configurations for each region. Correlation analysis is conducted to clarify flood risk relationships and to quantify how FRMP changes in one region influence others. Finally, the TOPSIS is used to evaluate all candidate solutions and identify the configuration that ensures coordinated flood risk management across regions.

2.1. Study area and data preparation

The Yangtze River Delta's Ecological Green Integration Demonstration Zone (Fig. 2) covers approximately 2413 km^2 across Qingpu District (Shanghai), Wujiang District (Suzhou, Jiangsu Province), and Jiashan County (Jiaxing, Zhejiang Province). By targeting inter-jurisdictional planning and governance challenges, the zone offers a suitable case for studying cross-regional flood risk management.

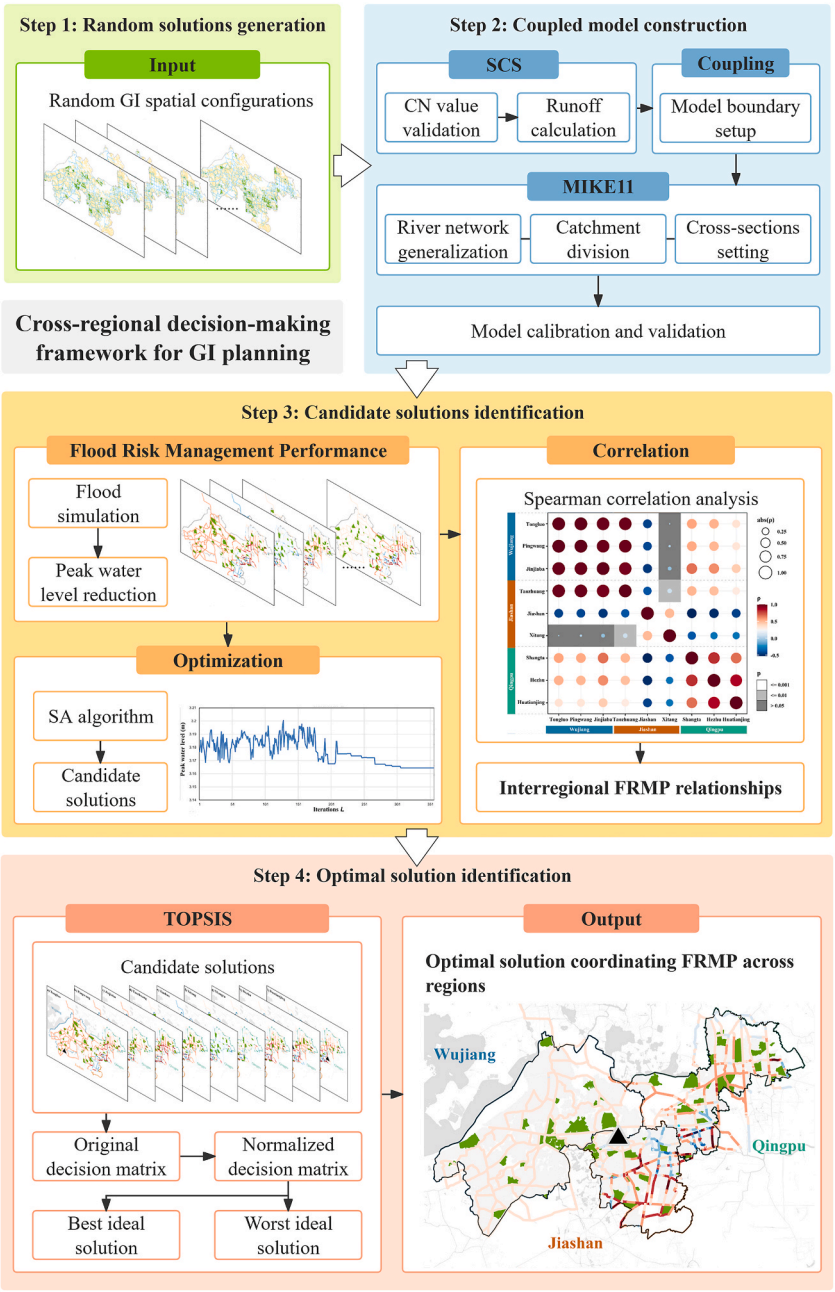

Fig. 1. A decision-making framework for coordinated GI planning for cross-regional flood risk management.

As the lowest-lying portion of the Yangtze River Delta (mean elevation <5 m) under a monsoon climate and a dense river–lake network, the area is highly flood-prone [47,49]. To mitigate flood risks, 332 polders covering 70.4 % of the study area (Fig. 3a), were established as primary catchments for flood management. This produces a dual hydrological regime: controlled storage-and-drainage within polders (operated by sluices and pumps once water depth exceeds maximum storage capacity) versus natural runoff processes in non-polder reaches [50].

Polders also introduce pronounced spatial heterogeneity in land-use patterns (e.g., area and configuration of GI, water-surface, and construction land) that modulate retention and regulation capacities, while reconfiguring hydrological connectivity across boundaries. These dynamics affect water levels in adjacent upstream and downstream river networks [47] and are particularly sensitive along provincial borders, where management disputes are frequently reported [46,48]. For example, polder consolidation in Wujiang altered the river-network configuration and reportedly raised water levels in Jiashan, increasing flood risk and impacting agriculture [46]. These cross-regional pressures underscore the need for coordinated flood risk management in the study area.

In this study, the main datasets included LULC, water system and cross-section data, hydraulic engineering maps, rainfall data, and hydrological boundary data. The 30m resolution LULC data from the Chinese Academy of Sciences was corrected using the 10m resolution ESA WorldCover dataset to improve accuracy for runoff calculations. Water system and cross-section data were sourced from local water conservancy annals and refined with DEM data. Hydraulic engineering maps provided the spatial distribution of dikes and pump stations across all polder catchments. Rainfall data from 21 stations and hydrological boundary data (water level, tide level, and discharge) from 20 stations were processed as time series files. Additional details, including data sources, time, format, and resolution, are provided in Table 1.

2.2. Random GI spatial configurations generation

In the study area, 98.78 % of farmland is paddy fields, characterized by saturated conditions and low infiltration due to impermeable clay layers; therefore, farmland was not classified as GI in this study. Consistent with the Territorial Planning for the Yangtze River Delta's Ecological Green Integration Demonstration Zone (2021–2035) —which (i) proposes converting selected rural polder areas to ecological land and (ii) sets a 4 % afforestation target—we operationalized GI expansion as farmland-to-woodland conversion within polders. The procedure was to randomly sample polder catchments and convert all farmland within selected catchments to woodland; if the cumulative woodland increase was still below 4 % of the study area, additional woodland was iteratively allocated to randomly chosen, previously unconverted polders until the 4 % target was reached, yielding randomized, policy-consistent GI layouts for scenario analysis.

2.3. SCS-MIKE11 coupled model construction

Simulating the infrastructure-mediated hydrological processes in plain river-network regions faces two key difficulties: (i) accurately representing human-regulated exchanges—sluice and pump operations, dike compartmentalization, and storage–release dynamics—between polder and non-polder catchments and the external river network; and (ii) coping with sparse and discontinuous

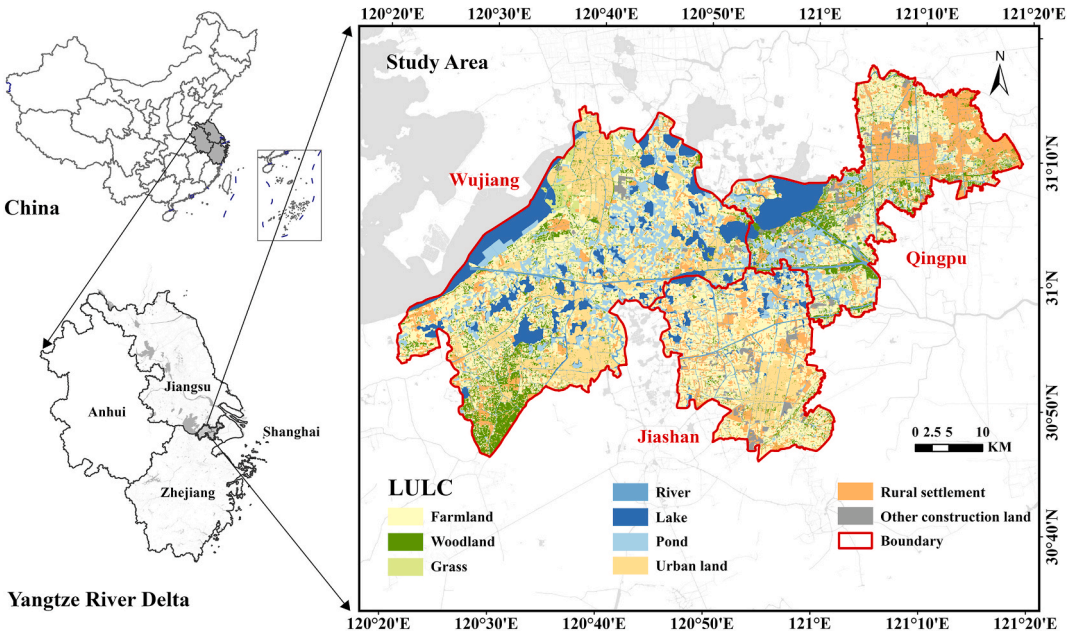

Fig. 2. Study area and LULC map in 2020.

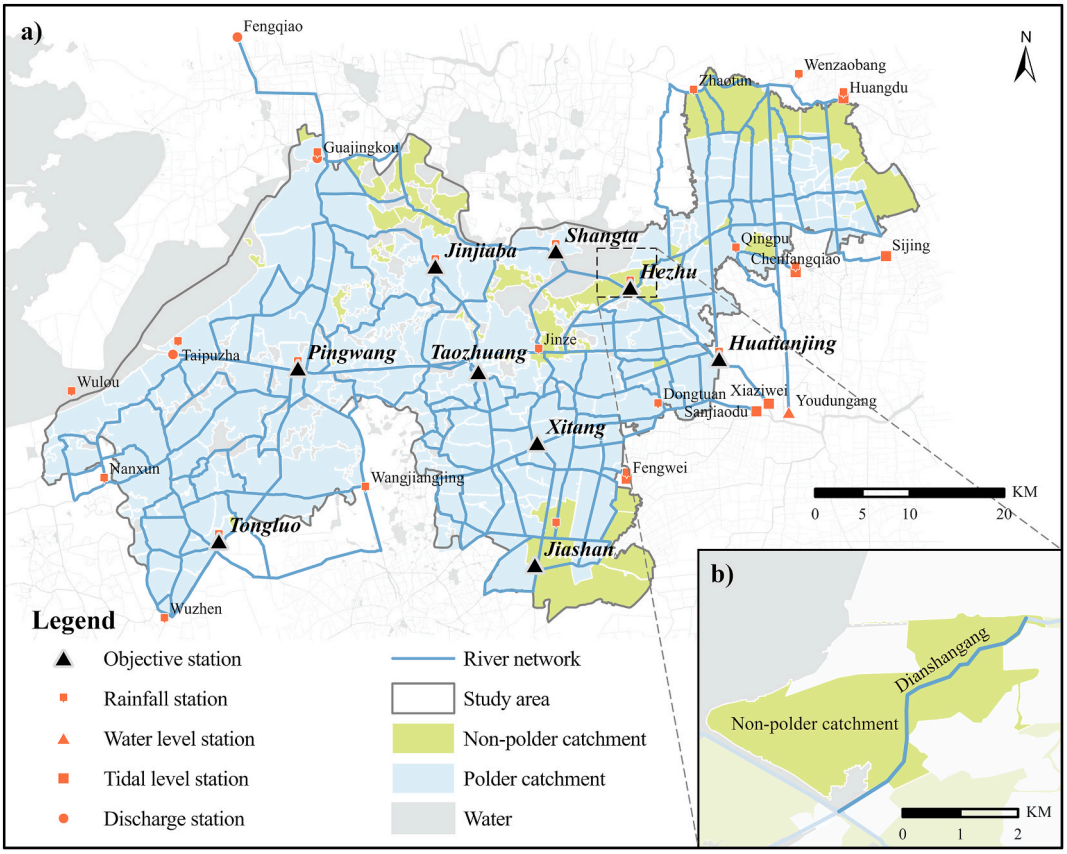

Fig. 3. SCS-MIKE11 model construction a) Catchment division and river network generalization; b) non-polder catchment delineation.

Table 1
Data sources.

Data types	Time	Format	Resolution	Data sources
LULC data	2020	Raster (.tif)	30m	Resource and Environment Science and Data Center, Chinese Academy of Sciences (http://www.resdc.cn/Default.aspx)
Land cover data	2020	Raster (.tif)	10m	ESA WorldCover Land Cover Dataset (https://esa-worldcover.org)
Water system and cross-section data	2000–2014	Excel (.csv)	/	Wujiang Annals, Wujiang Water Conservancy Annals, Jiayu Water Conservancy Annals, Qingpu Water Conservancy Annals
Hydraulic engineering maps	2019	Picture (.jpg)	1:50000	Wujiang District Water Resources Bureau, Jiashan County Water Resources Bureau, Qingpu District Water Resources Bureau
Rainfall and hydrological boundary data	2020	Excel (.csv)	Day	Zhejiang Provincial Department of Water Resources, Shanghai Water Authority, Jiangsu Provincial Hydrological and Water Resources Survey Bureau
DEM data	2022	Raster (.tif)	30m	Geospatial Data Cloud (https://www.gscloud.cn)

observations at numerous catchment outlets (discharge/water levels), which constrains calibration and validation of process-based models [50].

Process-based hydrological models (e.g., SWAT, SWMM, and MIKE SHE) can simulate runoff generation but typically require calibration and validation against observed data, which is difficult under these data constraints [51–53]. Hydrodynamic models (e.g., MIKE11 for 1-D river networks; MIKE21 for 2-D floodplains) capture unsteady routing and flood dynamics but do not generate catchment runoff on their own [54,55]. An integrated scheme is therefore needed, but its hydrological component must be data-light in this context.

This study accordingly used the Soil Conservation Service (SCS) model to estimate event runoff from precipitation and LULC with few parameters [56], and feed these lateral inflows into MIKE11 to simulate 1-D river-network hydraulics and exchanges with polder systems [53]. This SCS–MIKE11 coupling reproduces the key interactions in plain river network regions [50,53,57–59] and is well suited to evaluating how GI spatial configuration changes affect FRMP.

2.3.1. SCS model construction

This study employs the SCS model to calculate runoff for both polder and non-polder catchments. It can effectively capture the influence of different soil types, LULC patterns, and initial soil moisture conditions on rainfall-runoff processes. The runoff calculation formula is:

$$R = \begin{cases} \dfrac{(P - 0.05S)^2}{P + 0.95S}, P \geq 0.05S \\ 0, P < 0.05S \end{cases} \tag{1}$$

$$S = \frac{25400}{CN} - 254 \tag{2}$$

where R is the runoff depth (mm), P is precipitation (mm), S is potential maximum retention (mm) given by Eq. (2), and CN is SCS curve number, which is a function of a combination of soil, land use, and antecedent soil moisture condition (AMC). Each catchment was assigned to its nearest rainfall station using Thiessen polygon delineation, and precipitation data from the assigned station were used for runoff calculations (Supplementary Material Fig. S1).

Given that soil conditions in China differ from those in the US, this study calibrated CN values based on research in the Taihu Basin [60] to develop a set of CN values suitable for the study area (Supplementary Material Table S1). Soil moisture levels were determined using 5-day antecedent rainfall preceding a storm event. Based on AMC levels (Supplementary Material Table S2), CN values were assigned for dry, normal, and wet conditions. The calibration formulas are provided below:

$$CN_I = 4.2CN_{II} / (10 - 0.058CN_{II}) \tag{3a}$$

$$CN_{III} = 23CN_{II} / (10 + 0.13CN_{II}) \tag{3b}$$

The composite CN for each catchment was calculated as a weighted value based on the LULC type proportion. The actual runoff Q for each catchment was determined using Eq. (4):

$$Q = \frac{R \times A}{\Delta t} \tag{4}$$

where A is the catchment area (m^2), and Δt represents one day in seconds.

2.3.2. MIKE11 model construction

This study uses the MIKE11 model, a widely used one-dimensional hydrodynamic model for plain river network areas to simulate flood processes and generate data on water levels [54], which are subsequently used for FRMP calculations. Considering the flat terrain and dense water network characteristics of the study area, the river network system was digitized in ArcGIS. The numerous rivers and lakes were generalized into river networks and storage nodes, extending the model boundaries to discharge, water level, or tidal level stations (Fig. 3a). Upstream boundaries were set at three discharge stations (Fengqiao, Guajingkou, and Taipuzha), where discharge data were input as boundary conditions. Downstream boundaries were set at six tidal level stations (Huangdu, Sijing, Chenfangqiao, Xiaziwei, Sanjiaodu, and Fengwei) and one water level station (Youdungang), where tidal level and water level data were input as boundary conditions, respectively. For recorded rivers, the cross-sections were defined based on data from local water conservancy annals. For unrecorded rivers, the cross-sections were extracted and generalized into trapezoidal shapes based on water system data and DEM data.

2.3.3. SCS-MIKE11 coupled model setup

Based on the actual distribution of polders and the dispatch rules of pump stations in the study area, two types of catchments were delineated: polder and non-polder catchments. Polder catchments were delineated according to hydraulic engineering maps provided by local water resources bureaus. Non-polder areas were delineated into non-polder catchments based on proximity to the river network, facilitating subsequent calculations of outflow from catchments to the river network (Fig. 3b).

In polder catchments, the runoff routing process was deemed insignificant due to the small size and short distances involved. Therefore, the computed runoff volume R was directly applied to the water surface of the polder, leading to a change in water level as shown in Eq. (5):

$$\Delta H = \Delta H + \frac{R}{f} \tag{5}$$

where ΔH is the cumulative change in water depth (mm), R is the runoff depth (mm), and f is the water surface ratio of the polder.

When the cumulative water depth ΔH exceeds the maximum allowable storage depth of 200 mm, the drainage pump station in the polder is activated to discharge excess water into the external river network, after which ΔH is recalculated. If ΔH remains below the maximum allowable storage depth, no outflow occurs, and the water level within the polder remains unchanged.

For non-polder catchments, runoff routing followed the 4-4-2 rule from the Taihu Basin Model [61]:

$$Q_i(D3) = 0.4 \times Q(D1) + 0.4 \times Q(D2) + 0.2 \times Q(D3) \tag{6}$$

where $Q_i(D3)$ is the catchment outflow on the third day, and $Q(D1), Q(D2), Q(D3)$ are daily runoff values (m^3/s).

Flood discharge boundaries were set differently for polder and non-polder catchments: point source boundaries at pumping stations or sluices for polders, and distributed source boundaries around river networks for non-polder areas [50,53]. These settings allowed accurate simulation of runoff contributions to the river network during flood events.

2.3.4. Model accuracy

In the SCS-MIKE11 model, the initial roughness coefficient (Manning's n) was set to 0.03, which has been commonly used in Taihu Basin [62]. The initial water level was set to 2.80 m according to the average value of the local water level stations in June. Flood data from June 1 to 13 2020, was used for calibration, as it corresponded to a typical rainfall event, and the measured water levels during this time were close to the area's annual average. By comparing calculated water levels with measured water levels from 10 stations, the model parameters were further adjusted. Then the flood induced by Typhoon "Meihua" from September 12 to 24, 2020 was selected for validation and the model was evaluated with the commonly used metrics: correlation coefficient (R^2), root mean square error (RMSE) and Nash-Sutcliffe efficiency (NSE) [42,63]. Finally, the riverbed roughness coefficient ranged from 0.03 to 0.06, and the initial water level was adjusted to 3.00 m. Validation results showed $R^2 = 0.874$, RMSE = 0.123, and NSE = 0.840, indicating high model accuracy suitable for further analysis (see Supplementary Material Fig. S2).

2.4. Candidate solutions identification

2.4.1. FRMP optimization objective setting

The heavy rainfall event from June 14 to 28, 2020, was used to simulate flood processes under random GI spatial configurations (Supplementary Material Table S3). Measured discharge, tidal level, and water level data at boundary stations from June 16 to 28, 2020, were used as input boundary conditions in MIKE11 model (Supplementary Material Tables S4–6). Three representative stations were selected within each of the three regions—Wujiang, Jiashan, and Qingpu (Fig. 3a). Since watershed flood risk is typically correlated with peak river runoff [50,64,65], this study adopted peak water level reduction as the indicator for evaluating FRMP. Each optimization iteration targeted the peak water level reduction at one of the selected representative stations as the optimization objective, with the objective function defined as follows:

$$Maximize: f(S) = \Delta H_P = H_p(S_0) - H_p(S) \tag{7}$$

where ΔH_P is the peak water level reduction (m), $H_p(S_0)$ is the peak water level under the initial GI spatial configuration S_0 (m), and $H_p(S)$ is the peak water level under the new GI spatial configuration S (m).

2.4.2. SA construction and optimization

SA, a heuristic algorithm, was applied to handle the large number of spatial configurations involved in GI optimization [66,67]. SA enhances solution diversity and avoids local optima, making it suitable for identifying global optima. The optimization process in this study (see Supplementary Material Fig. S3) began with randomly generated GI spatial configurations (Section 2.2) and iteratively perturbed solutions by reallocating woodland among polder catchments.

Perturbations involved: a) randomly selecting two polder catchments where all farmland was converted to woodland, and one polder catchment where partial conversion occurred; b) undoing these changes and reallocating woodland as per Section 2.2.

SA parameters were set as follows: an initial temperature of 100, 500 iterations, a cooling rate of 0.90, and a concave cooling function. The optimization process terminated when 50 consecutive solutions were rejected, and the temperature dropped below 0.001. During each iteration, the SCS-MIKE11 coupled model simulated peak water level reductions under different GI configurations, and SA evaluated these results to identify the optimal configurations as candidate solutions.

2.4.3. Interregional FRMP correlation analysis

To assess interregional FRMP relationships, all GI configurations generated during SA iterations were analyzed. First, Spearman rank correlation of analysis was applied to identify monotonic relationships between FRMP across representative stations, as this non-parametric method can detect consistent directional trends regardless of whether the relationship is linear or nonlinear [68]. Second, since locally weighted scatterplot smoothing (LOWESS) regression can effectively capture complex nonlinear patterns and local variations in data relationships without assuming specific functional forms [69], it was employed to reveal potential thresholds and nonlinear relationships that Spearman correlation analysis alone cannot detect, thereby clarifying how FRMP improvements in one region influence neighboring regions.

The fundamental principle of LOWESS is to perform locally weighted least squares regression on observed data points near the target point, generating smooth predicted values [69]:

$$\hat{y}(x) = \widehat{\beta_0}(x) + \widehat{\beta_1}(x)x \tag{8}$$

where $\widehat{\beta_0}(x)$, $\widehat{\beta_1}(x)$ are obtained by minimizing the following weighted sum of squared residuals:

$$\min_{\beta_0,\beta_1} \sum_{i=1}^{n} \omega_i(x)(y_i - \beta_0 - \beta_1 x_i)^2 \tag{9}$$

where $\omega_i(x)$ is the weight function that depends on the distance between the data point x_i and the target point x:

$$\omega_i(x) = \begin{cases} \left(1 - \left|\frac{x - x_i}{h}\right|^3\right)^3, |x - x_i| \le h \\ 0, |x - x_i| > h \end{cases} \tag{10}$$

where h is the bandwidth that controls the neighborhood size.

Third, to quantify the interregional benefit distribution, the FRMP distribution across all river cross-sections in each region (13,229 cross-sections in total) under each candidate solutions was statistically analyzed.

2.5. Optimal solution decision-making with TOPSIS

The TOPSIS method, a multi-criteria decision analysis approach, was used to evaluate candidate solutions relative to a set of assessment criteria [70]. It assesses each solution based on its proximity to the best ideal solution (BIS) and distance from the worst ideal solution (WIS). This study constructed a decision matrix x_{ij} using FRMP values from all representative stations under each candidate solution (Supplementary Material Table S7). Since FRMP is a positive indicator, the decision matrix was normalized using Eq. (11):

$$r_{ij} = \frac{x_{ij} - min\ x_{ij}}{max\ x_{ij} - min\ x_{ij}} \tag{11}$$

where r_{ij} is the normalization matrix; x_{ij} is the FRMP value of station j under candidate solution i. TOPSIS scores, calculated using the formulas below, were then used to identify the optimal solution that balances FRMP across regions.

$$S_i^+ = \sqrt{\sum_{j=1}^{n} \left(r_{ij} - r_j^+\right)^2} \tag{12a}$$

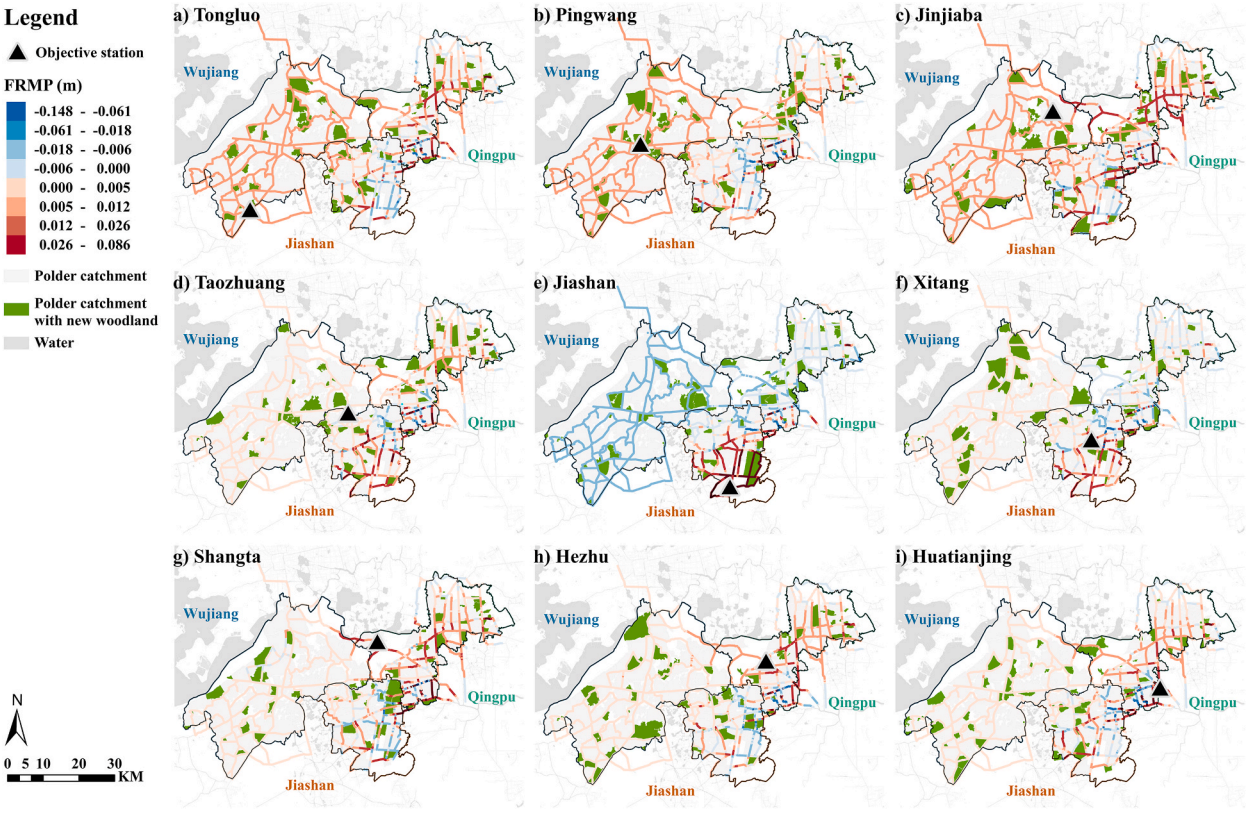

Fig. 4. Optimized GI spatial configurations and corresponding FRMP distributions across candidate solutions.

$$S_i^- = \sqrt{\sum_{j=1}^{n} \left(r_{ij} - r_j^-\right)^2} \tag{12b}$$

$$T_i = \frac{S_i^-}{S_i^+ - S_i^-} \tag{13}$$

where S_i^+, S_i^- are the distance of candidate solution i to BIS and WIS, respectively; and T_i is the closeness coefficient also as TOPSIS score. BIS and WIS are defined as follows:

$$BIS = \left(r_1^+, r_2^+, \cdots, r_j^+\right), r_j^+ = max\left\{r_{1j}, r_{2j}, \cdots, r_{ij}\right\} \tag{14a}$$

$$WIS = \left(r_1^-, r_2^-, \cdots, r_j^-\right), r_j^- = min\left\{r_{1j}, r_{2j}, \cdots, r_{ij}\right\} \tag{14b}$$

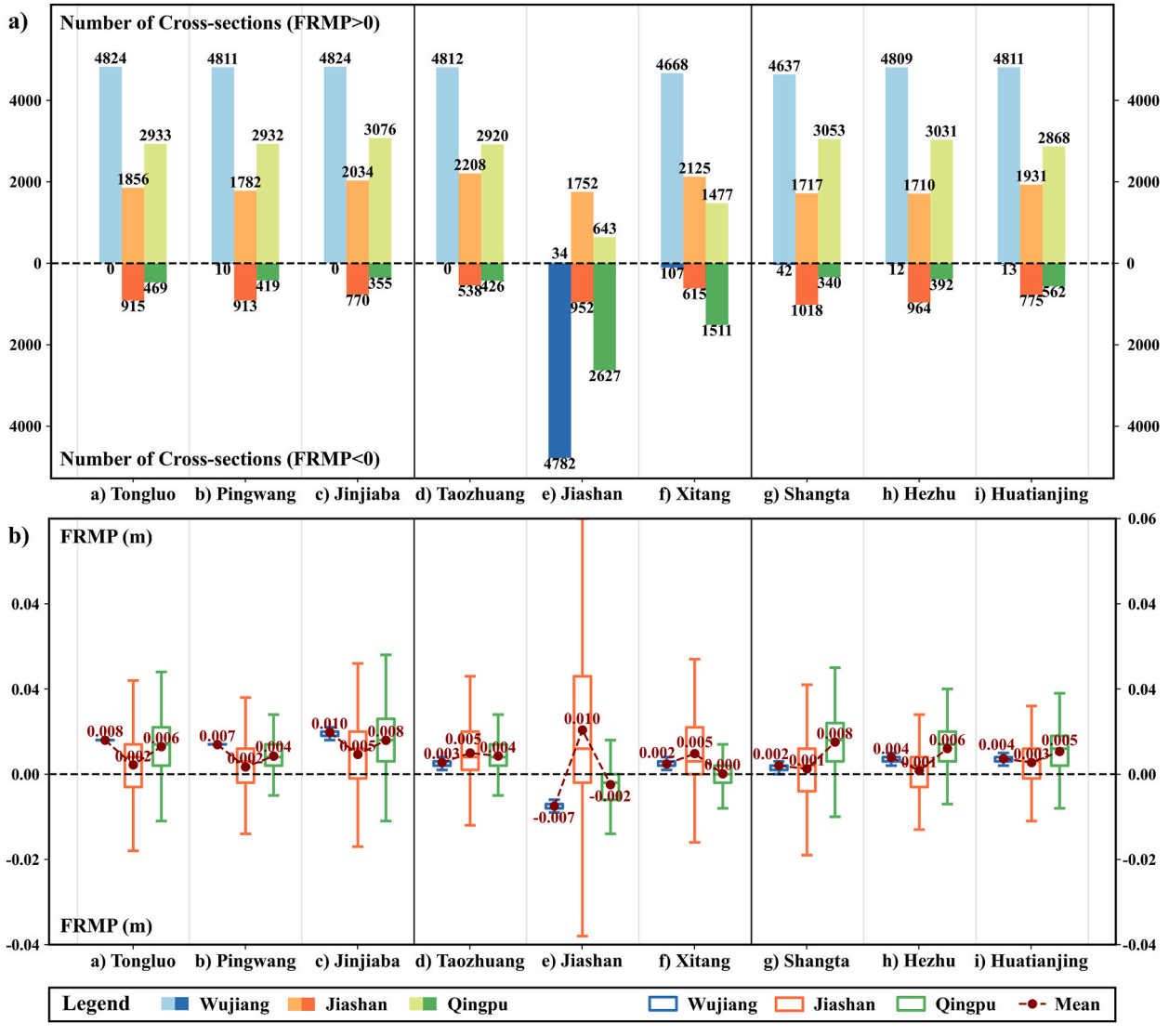

Fig. 5. Regional flood risk reductions under candidate solutions: a) Cross-section counts for FRMP improvements and deteriorations; b) Distribution of FRMP values across cross-sections by region.

3. Results

3.1. Candidate solutions and optimization results

Our results, as shown in Supplementary Material Fig. S4, demonstrate the effectiveness of the SA algorithm. In one iteration of candidate solution i), the algorithm began with an initial peak water level of 3.182 m. During the early optimization stages, the high algorithmic temperature enabled the acceptance of suboptimal solutions, which led to significant fluctuations in peak water levels—occasionally exceeding 3.2 m. As the temperature decreased, the algorithm stabilized and ultimately converged to the global optima, reducing the peak water level by approximately 1.76 cm. This process enabled the identification of nine candidate optimal GI spatial configurations, each tailored to reduce peak water levels at representative stations in Wujiang, Jiashan, and Qingpu regions (Fig. 4). Notably, regardless of the optimization objective, the resulting GI spatial configurations consistently exhibited a dispersed pattern, even though the FRMP distribution varied substantially across the candidate solutions.

To further assess the impact of these configurations, candidate solutions were evaluated based on their FRMP. Solutions optimized for individual regions significantly improved local FRMP but produced limited or even adverse effects on adjacent regions. For instance, candidate solutions targeting Wujiang (a-c) achieved effective local peak water level reductions. Across these solutions, over 4811 cross-sections within Wujiang experienced decreases in peak water levels, with an average reduction exceeding 0.007 m (Fig. 5). However, improvements in Jiashan and Qingpu were modest—averaging just over 0.002 m and 0.004 m, respectively—with candidate solutions b and c even increasing peak water levels in 770 cross-sections in Jiashan and 355 cross-sections in Qingpu. This clearly indicates that an upstream-focused strategy may not sufficiently address downstream flood risks and could inadvertently intensify vulnerabilities in midstream regions.

A similar pattern of trade-offs was observed in other candidate solutions. Notably, candidate solution e, which targeted Jiashan, demonstrated substantial local benefits with an average FRMP improvement exceeding 1 cm. Yet, these gains came at the cost of increasing peak water levels upstream in Wujiang (with 4782 affected cross-sections and an average increase of exceeding 0.007 m)

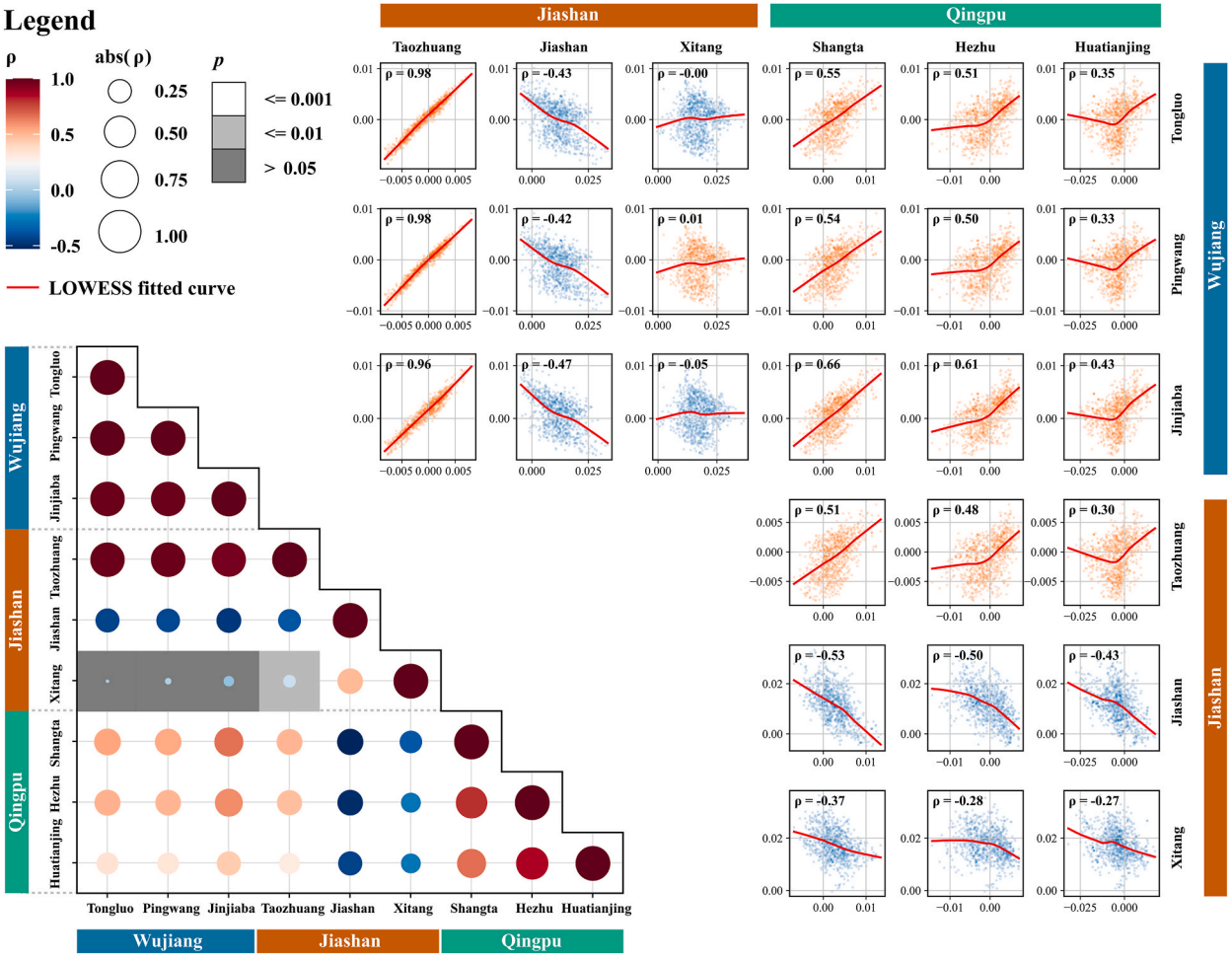

Fig. 6. Correlation analysis (Spearman's rank correlation coefficients) and LOWESS regression of FRMPs across regions.

and downstream in Qingpu (with 2627 affected cross-sections and an average increase of over 0.002 m). Such findings underscore that optimizing for a single region may disrupt upstream hydrological dynamics and exacerbate interregional conflicts.

In contrast, candidate solutions focusing on downstream regions, such as those for Qingpu (g–i), demonstrated a more balanced interregional impact. While these solutions achieved significant local improvements—reducing peak water levels in over 2868 cross-sections and yielding an average FRMP improvement exceeding 0.005 m—the benefits to Wujiang and Jiashan were more modest, with average improvements not exceeding 0.004 m and 0.003 m, respectively.

In summary, the optimization results demonstrate that strategies targeting individual regions primarily enhance local FRMP but fall short of delivering balanced improvements across the entire watershed. Midstream-focused strategies (e.g., candidate solution d-f) tend to intensify interregional trade-offs, whereas upstream (e.g., candidate solution a-c) or downstream strategies (e.g., candidate solution g-i) offer greater potential for cross-regional flood risk mitigation. These findings highlight the need for a cross-regional approach to GI planning that can balance localized benefits with broader watershed management.

3.2. *Correlation analysis and LOWESS regression results*

During the iterative process of all candidate solutions, 944 GI spatial configurations were generated, enabling correlation analysis of regional FRMPs (Fig. 6). The analysis revealed significant flood risk interactions across regions. The FRMP correlation coefficients for Wujiang and Qingpu are higher than those for midstream Jiashan, suggesting stronger intra-regional relationships in upstream and downstream region. Upstream Wujiang and downstream Qingpu exhibited positive FRMP correlations (p <0.001), while Jiashan showed a negative correlation with Qingpu, suggesting significant interregional relationships (p <0.001).

Spearman's rank correlation coefficients further quantified these interactions. Among upstream and downstream regions, Jinjiaba and Shangta showed the strongest positive correlation ($\rho = 0.66$). Among midstream and downstream regions, Jiashan and Shangta exhibited the strongest negative correlation (ρ = -0.53). Notably, the correlation between Wujiang and Qingpu, as well as between Wujiang and Jiashan, was more significant (with larger $|\rho|$ values) when the stations were closer to the regional boundaries. Interestingly, Taozhuang station, located at the Wujiang-Jiashan boundary, demonstrated a stronger FRMP correlation with Wujiang ($|\rho|$ >0.96) than with Jiashan ($|\rho|$ <0.48), indicating that its FRMP was more strongly influenced by upstream regions.

LOWESS regression revealed richer nonlinear relationships between regional flood risks during flood events. Many station pairs exhibited threshold effects in their FRMP relationships. For example, Hezhu station in Qingpu showed a positive correlation pattern with the three stations in Wujiang that changed at approximately Hezhu's FRMP = −0.002 m.When Hezhu's FRMP exceeded this threshold, Wujiang's FRMP improved significantly, suggesting potential synergistic effects rather than direct causation. Furthermore,

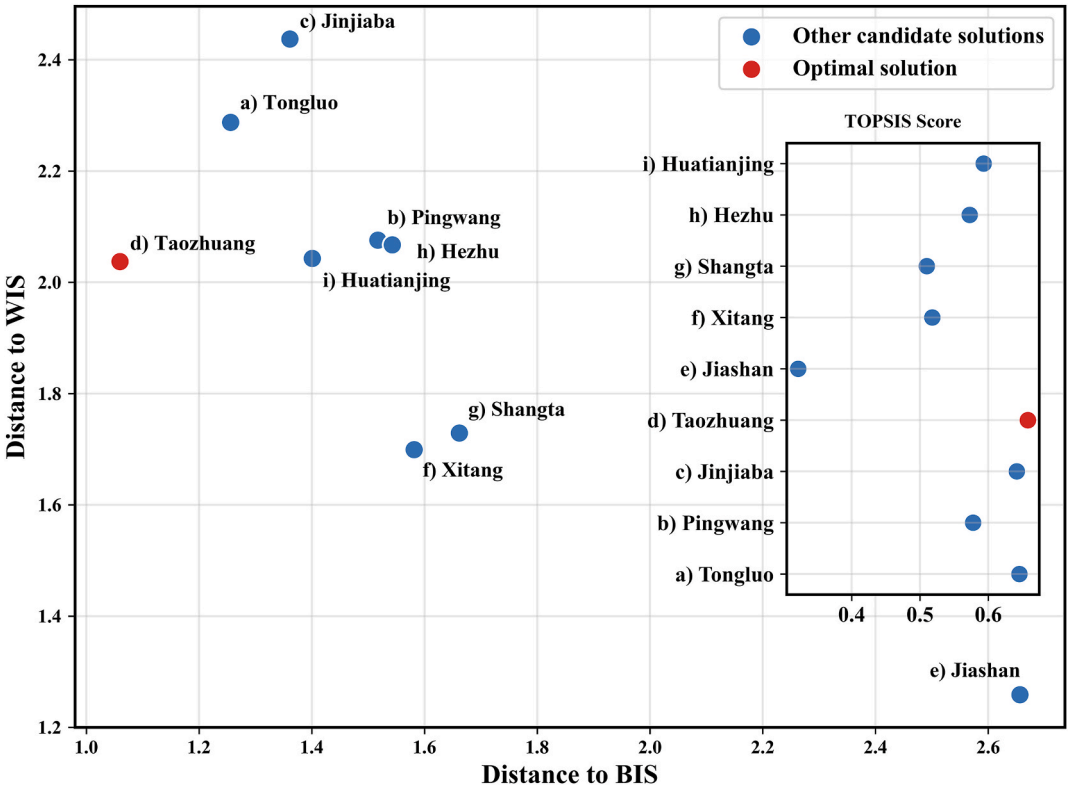

Fig. 7. Distances to BIS/WIS and TOPSIS score for nine candidate solutions.

the relationship between Huatianjing station and the three stations in Wujiang shifted from negative to positive when Huatianjing's FRMP reached approximately −0.005 m, indicating complex nonlinear interactions between watershed outlet and upstream flood risks. However, although LOWESS regression showed more complex nonlinear interaction patterns, Spearman analysis still confirmed certain monotonic correlations between regions (such as between Wujiang and Qingpu, $|\rho| \geq 0.33, p < 0.001$). Thus, enhancing FRMP in downstream Qingpu may mitigate risks in upstream Wujiang but exacerbate risks in Jiashan.

3.3. TOPSIS assessment results

The TOPSIS method was applied to evaluate the nine candidate solutions (see Supplementary Material Table S8). Candidate solution d emerged as the optimal solution, achieving a TOPSIS score exceeding 0.65. Solutions a–c and i also performed relatively well, while solution e, focused on Jiashan, scored the lowest (Fig. 7).

Specifically, candidate solution d targeted peak water level reductions at Taozhuang station, effectively balancing FRMP improvements across Wujiang, Jiashan, and Qingpu regions. Since Taozhuang is located at the Wujiang-Jiashan boundary, optimization targeting Taozhuang mitigated flood risks both upstream Wujiang and midstream Jiashan. Furthermore, based on the result in Section 3.2, reductions at Taozhuang mitigated flood risks in downstream Qingpu, thereby enhancing the FRMP of the entire watershed. It demonstrates that optimizing at regional boundaries leverages these points as natural outflow controls, thereby reducing flood risks across the entire watershed system. Moreover, solutions targeting the watershed outlet (e.g., Huatianjing) or upstream regions (e.g., Jinjiaba), yields moderate benefits—outlets regulate runoff at hydrological endpoints, and upstream interventions reduce it at the source—an approach particularly suited to large watersheds [71–73].

These findings highlight the effectiveness of boundary-focused optimizations in achieving balanced FRMP improvements through cross-regional hydrological interactions. They emphasize the need for integrated strategies to address trade-offs and ensure comprehensive watershed flood risk management.

4. Discussion

4.1. GI spatial configuration optimization responds to watershed heterogeneity

Optimizing GI spatial configurations has been central to flood risk management research [27,74]. While numerous studies have sought universal planning rules to mitigate flooding across multiple scales, they frequently yield different conclusions [75–78]. Watershed-scale investigations reveal that heterogeneity stemming from variations in terrain, soils, land use and hydrological connectivity [37,38] likely accounts for these divergent findings. Despite this variability, many of these investigations predominantly advocate clustered layouts—either placing GI along river corridors [39–41] or concentrating it in downstream areas [42].

These prescriptions, however, address only coarse watershed-scale heterogeneity and overlook finer-scale variability in soil properties, land-use patterns and hydrological connectivity [79], resulting in spatially varying GI effectiveness across individual grid cells. To address this gap, grid-cell–level studies have demonstrated that dispersed configurations consistently outperform clustered layouts under heterogeneous conditions [1]. Our results corroborate Chen et al. [1], further indicating that dispersed layouts more effectively accommodate finer-scale heterogeneity.

To operationalize this finding, we captured heterogeneity and infrastructure-mediated hydrological connectivity in the modeling framework. We incorporated spatially varying land-use and soil-types into CN—based runoff calculations, with composite CN values reflecting catchment-level land-use patterns. We also incorporated the impacts of grey infrastructure on hydrological connectivity by distinguishing between polder and non-polder hydrology processes: representing polders as dike-bounded catchments with internal storage accounting, where exchanges with the river network occur only via rule-based pumps and sluices. These distinct processes were simulated through SCS–MIKE11 coupling to reflect actual hydrological connectivity [50]: rule-based point-source boundaries at pumping stations and sluices for polder catchments—through which runoff is discharged to the external river network when the cumulative depth exceeds the allowable storage threshold—and distributed lateral-inflow boundaries along river links for non-polder catchments, whose runoff disperses directly into the river network. After SA optimization, dispersed GI layouts more effectively attenuate flood peaks and modulate watershed dynamics than clustered arrangements. A comparison with Gabriels et al. [40] underscores the role of hydrological connectivity: although they similarly applied SCS at the grid-cell scale—accounting for soil and land-use variability—their omission of grey-infrastructure effects limited their model to topography-driven flows and led to a preference for corridor placement. By explicitly modeling both natural and infrastructure-mediated flows, our approach provides a more comprehensive representation of hydrological connectivity and thus a stronger, context-sensitive basis for optimizing GI spatial configurations.

Building on these findings, our adaptive GI spatial optimization provides a basis to tailor GI strategies to heterogeneous upstream–downstream contexts within a watershed. Consistent with Kato and Huang [80], who advocate hybrid GI—downstream urban interventions coupled with upstream ecosystem management across differing land uses—our fine-scale heterogeneity analysis enables the precise siting of strategically configured GI layouts that complement such hybrid approaches. This also aligns with our dispersed GI spatial optimization logic, providing a practical template for designing upstream–downstream strategies.

Therefore, given pervasive watershed heterogeneity, flood risk management should move beyond a single, uniform rule for GI planning and adopt more adaptive optimization strategies grounded in fine-scale variability.

4.2. A response to the global challenge of cross-regional flood risk management

4.2.1. Promote distributive justice: balancing interregional benefits and burdens

Cross-regional flood risk management is a persistent global challenge, largely due to the transboundary nature of many major rivers and resultant coordination issues [6]. Even within non-transboundary watersheds, the lack of interregional coordination can cause localized flood mitigation efforts to inadvertently increase risks of other regions [81,82]. Our study, along with investigations in Vietnam's Mekong Delta [16] and in the Ganges-Brahmaputra-Meghna, Mahanadi, and Volta deltas [20], illustrates these adverse effects. When interregional flood risk relationships are unclear, coordination falters. This produces an uneven distribution of benefits and burdens—a central distributive justice concern in flood risk management [83]—where those who bear the burdens are not those who receive the benefits [84].

In many watersheds, upstream regions shoulder primary burdens, including constructing grey infrastructure (e.g., dams and reservoirs) to mitigate watershed-wide flooding and implementing ecosystem management to enhance ecological benefits [85]. Downstream regions, by contrast, avoid these burdens while benefiting from upstream measures [8]. Such asymmetries can trigger interregional conflicts. For example, Bulgaria, located upstream of the Maritsa River, has historically been reluctant to construct joint dams with Turkey due to funding and land rights issues [85]. Moreover, upstream measures do not necessarily benefit downstream regions: upstream dike construction can increase peak water level [16] and reduce biodiversity and ecosystem productivity downstream [22], further complicating these conflicts. Accordingly, resolving benefit-burden distribution issues requires clearly establishing interregional flood risk relationships. However, the absence of an empirically validated model for predicting these relationships across regions impedes robust coordination. To address this gap, this study quantifies interregional FRMP relationships, revealing a significant negative correlation between flood risks in Wujiang and Jiashan regions ($|\rho| \geq 0.21$, $p < 0.001$). This finding aligns with historical flood events during the 1950s–1960s: while Wujiang's polder system construction reduced local flood risks and increased agricultural yields, it simultaneously elevated flood risks in Jiashan, severely affecting agricultural productivity and provoking persistent water resource disputes between the two regions [46]. By making these interregional relationships explicit, our framework enables evidence-based negotiations among stakeholders of different regions.

To facilitate the negotiation of burdens and benefits, watershed-wide cooperation offers a practical pathway. European practice demonstrates shifts in decision-making toward multiple regional authorities and non-state stakeholders. In Scotland and England, the catchment-scale approach extends flood risk management beyond narrow urban focuses to catchment-scale and encourages local actors to engage in flood risk policies [86]. Austria's watershed-wide management plans similarly emphasize upstream-downstream cooperation between national and local authorities [84,87]. Such arrangements broaden participation and strengthen interregional coordination.

Additionally, equitable fiscal allocation and economic compensation mechanisms can help balance burdens and benefits among stakeholders. Machado et al. [88] demonstrate that in Salvador/Bahia, Brazil, substantial financial resources were misallocated to expensive grey infrastructure construction in high-income areas, while low-income areas received only cheap, ineffective temporary measures, exposing them to higher risks. By contrast, Indian watershed projects innovatively adopted a mechanism whereby downstream landholders compensate landless people upstream to share benefits [89]. Furthermore, taxation mechanisms [90] can be designed according to the actual costs incurred and benefits received by each region in reducing flood risk, compensating high-investment regions via levies on high-benefit regions.

4.2.2. Integrated land and water management

Cross-regional flood risk coordination has largely relied on traditional grey infrastructure strategies—such as dam construction, exemplified by the Maritsa Basin collaboration among Greece, Turkey, and Bulgaria [85]—which prioritizes immediate economic and protective benefits such as flood control and hydropower generation while potentially leading to long-term ecological degradation and secondary impacts like increased sedimentation, further exacerbating interregional disputes [20]. As a complement, coordinated GI planning offers a nature-based solution that mitigates flood risk and delivers ecological co-benefits. Although primarily urban and city-regional in scope, the EU GREEN SURGE project is cited here not as a basin-scale flood initiative, but as an institutional model of multi-actor coordination, shared standards, and learning platforms for organizing GI across jurisdictions [91].

At the watershed scale, Kato and Huang [80] advance a hybrid GI paradigm that embeds hydrologic objectives in land-use decisions: downstream urban areas with high water tables prioritize storage and evapotranspiration (e.g., added GI), whereas upstream areas emphasize maintaining forest ecosystems to delay and attenuate flood peaks. This study operationalizes that paradigm through a cross-regional decision framework that (i) harmonizes indicators and land-use metrics, (ii) allocates GI measures spatially across jurisdictions, and (iii) optimizes portfolios for flood-risk reduction and co-benefits. Translating such a paradigm into practice depends on enabling institutions capable of coordinating land-use decisions, common standards, and cost-sharing across administrative boundaries, amid land management complexities that have hindered cross-regional application [23,92].

Against this institutional backdrop, China established the Yangtze River Delta Ecological Green Integration Demonstration Zone in 2019 to coordinate interregional management through unified territorial planning [93], with GI planning constituting an essential component of land management. Yet implementation remains misaligned with the above coordination logic: planning efforts remain fragmented, with regions assigned individual GI targets rather than pursuing a strategically coordinated, portfolio-based allocation [94]. This gap motivates a decision-making framework capable of optimizing GI planning for cross-regional flood risk management. The Demonstration Zone's cross-regional territorial planning initiatives provide a platform for applying our framework, enhancing its practical applicability. By optimizing land-use decisions with explicit flood risk objectives, the framework integrates water and land management. This integration is further validated by our observation of a dispersed GI spatial configuration, demonstrating the

effectiveness of coordinated land management in achieving robust integrated water resources management [95–97]. In contrast, many cross-regional coordination efforts face challenges due to separately managed water and land systems such as Austria's Aist cooperation [15] and the Maritsa Basin collaboration [85], where the critical need for integrated management is often overlooked.

In summary, our research provides a robust framework for two complementary pathways—balancing interregional benefits and burdens, and integrating water and land management—to address the global challenge of cross-regional flood risk management.

4.3. Limitations of the study

While this study provides robust decision-making support for cross-regional GI planning to manage flood risks, several limitations warrant acknowledgment. First, the spatial context and scenario design impose certain constraints. The findings, derived from flat plain region of the Yangtze River Delta, may not be directly applicable to regions with varying terrain. Future research should validate these results across diverse topographical settings. Second, the hydrological model used in this study—the SCS model—introduces certain limitations. Under fixed land use component configurations, the location of GI within a catchment does not influence runoff generation, meaning that randomly generated GI configurations cannot achieve grid-scale precision. With the emergence of machine learning methods, these limitations stemming from insufficient observed data could be mitigated [4]. For example, XGBoost machine learning model can be used to predict grid-scale flood risks [63]. Such advancements hold promise for developing more accurate models and achieving finer-scale GI planning. Third, permanent basic farmland was not precisely excluded from conversion in the GI spatial configuration optimization. Future research with access to precise permanent basic farmland data could incorporate these areas as conversion constraints, making GI spatial configurations generation more realistic and policy-compliant. Lastly, the solutions identified in this study do not take economic feasibility into consideration. Future research should integrate GI construction costs and other economic factors to meet the needs of policymakers. But using TOPSIS as the decision-making model allows us to integrate costs into multi-objective decision-making frameworks [70,98].

Furthermore, our study proposes a novel location-focused optimization strategy: optimal GI spatial configurations should be derived from performance at critical locations—particularly regional boundaries—as primary optimization objectives. By relying on flexible optimization target selection rather than a singular GI planning rule, this strategy offers greater feasibility across diverse contexts. However, the conclusion that regional boundaries serve as optimal targets for GI optimization requires validation in other geographical and hydrological contexts to establish its broader applicability and generalizability.

5. Conclusion

This study presents a novel decision-making framework for coordinated GI planning that not only enhances watershed FRMP but also equitably balances benefits across regions. Using the Yangtze River Delta's Ecological Green Integration Demonstration Zone as a case study, our work offers valuable insights and practical tools for decision-makers and planners. Our findings demonstrate that prioritizing the FRMP of critical locations—especially at regional boundaries—as optimization objectives is key to mitigating flood risks across regions. Furthermore, our results reveal that optimal GI spatial configurations are dispersed rather than clustered, challenging conventional placement strategies. Crucially, our approach diverges from traditional models by adopting an equitable framework, ensuring that benefits are distributed fairly across all regions. To operationalize such equity in practice, watershed-wide cooperation and economic compensation mechanisms offer viable pathways. This integrated approach, which aligns land management with water management within an existing cross-regional territorial framework, underscores the importance of synchronizing these systems to achieve effective integrated water resources management.

In summary, by accounting for watershed heterogeneity and employing multi-objective decision-making, our study enhances the theoretical framework of coordinated GI planning and offers a nature-based approach to addressing the global challenge of cross-regional flood risk management.

CRediT authorship contribution statement

Qichen Hong: Writing – review & editing, Writing – original draft, Visualization, Validation, Software, Methodology, Investigation, Formal analysis, Data curation, Conceptualization. **Haoxun Zhang:** Validation, Software, Methodology, Investigation, Funding acquisition. **Bin Chen:** Supervision. **Steffen Nijhuis:** Writing – review & editing. **Yuting Xie:** Writing – review & editing, Writing – original draft, Supervision, Funding acquisition, Conceptualization.

Declaration of generative AI and AI-assisted technologies in the writing process

During the preparation of this work the authors used ChatGPT and Claude in order to improve the readability and language coherence of the manuscript. After using this tool, the authors reviewed and edited the content as needed and take full responsibility for the content of the published article.

Declaration of competing interest

The authors declare that they have no known competing financial interests or personal relationships that could have appeared to influence the work reported in this paper.

Acknowledgements

This work was supported by the Natural Science Foundation of Zhejiang Province [grant number LQ21E080016] and the Scientific Research Fund of Zhejiang Provincial Education Department [grant number Y202352584]. This work was also supported by the research project [grant number S-20250011] funded by the Architectural Design & Research Institute of Zhejiang University Co., Ltd. The authors gratefully acknowledge the Zhejiang Provincial Department of Water Resources, the Shanghai Water Authority, and the Jiangsu Provincial Hydrological and Water Resources Survey Bureau for providing observed hydrological and hydrodynamic data. We also thank the Jiashan County Water Resources Bureau, the Qingpu District Water Resources Bureau, and the Wujiang District Water Resources Bureau for sharing essential hydraulic engineering maps. Their support was instrumental in conducting this research.

Appendix A. Supplementary data

Supplementary data to this article can be found online at https://doi.org/10.1016/j.ijdrr.2025.105856.

Data availability

Data will be made available on request.

References

[1] H. Chen, Y. Dong, H. Li, Optimized green infrastructure planning at the city scale based on an interpretable machine learning model and multi-objective optimization algorithm: a case study of central Beijing, China, Landsc. Urban Plann. 252 (2024) 105191, https://doi.org/10.1016/j.landurbplan.2024.105191.
[2] T. Xu, K. Yu, D. Li, M. Wang, Assessment and impact factor analysis on stormwater regulation and storage capacity of urban green space in China and abroad, China City Plan. Rev. 32 (2023), https://doi.org/10.20113/j.ccpr.2023.01.001.
[3] IPCC, AR6 Synthesis Report: Climate Change, 2023 (n.d.), https://www.ipcc.ch/report/ar6/syr/. (Accessed 14 April 2025).
[4] J. Chen, G. Huang, W. Chen, Towards better flood risk management: assessing flood risk and investigating the potential mechanism based on machine learning models, J. Environ. Manag. 293 (2021) 112810, https://doi.org/10.1016/j.jenvman.2021.112810.
[5] Z. Luo, J. Tian, J. Zeng, F. Pilla, Resilient landscape pattern for reducing coastal flood susceptibility, Sci. Total Environ. 856 (2023) 159087, https://doi.org/10.1016/j.scitotenv.2022.159087.
[6] UNEP-DHI, UNEP, TWAP, Transboundary River Basins: Status and Trends (2016). http://geftwap.org/publications/river-basins-technical-report.
[7] C.L. Pandey, J. Joseph, R. Deshar, P. Niraula, Transboundary flood resilience: insights from Narayani and Mahakali Basins, Int, J. Disaster Risk Reduct. 86 (2023) 103535, https://doi.org/10.1016/j.ijdrr.2023.103535.
[8] N. Gupta, S. Dahal, A. Kumar, C. Kumar, M. Kumar, A. Maharjan, D. Mishra, A. Mohanty, A. Navaraj, S. Pandey, A. Prakash, E. Prasad, K. Shrestha, M. S. Shrestha, R. Subedi, T. Subedi, R. Tiwary, R. Tuladhar, A. Unni, Rich water, poor people: potential for transboundary flood management between Nepal and India, Curr. Res. Environ. Sustain. 3 (2021) 100031, https://doi.org/10.1016/j.crsust.2021.100031.
[9] F. Lara-Valencia, M. Garcia, L.M. Norman, A. Anides Morales, E.E. Castellanos-Rubio, Integrating urban planning and water management through green infrastructure in the United States-Mexico border, Front. Water 4 (2022), https://doi.org/10.3389/frwa.2022.782922.
[10] UNESCO, UNECE, Progress on Transboundary Water Cooperation: Mid-Term Status of SDG Indicator 6.5.2, with a Special Focus on Climate Change, UNESCO, 2024, https://doi.org/10.54677/QMQX8780.
[11] L. Leng, H. Jia, A.S. Chen, D.Z. Zhu, T. Xu, S. Yu, Multi-objective optimization for green-grey infrastructures in response to external uncertainties, Sci. Total Environ. 775 (2021) 145831, https://doi.org/10.1016/j.scitotenv.2021.145831.
[12] Y. Liu, W. Qi, M. Li, S. Wu, J. Pang, Z. Zhao, A conceptual framework for implementing green-grey infrastructures to mitigate urban flood through source-to-hazard intervention pattern, Int. J. Disaster Risk Reduct. (2025) 105432, https://doi.org/10.1016/j.ijdrr.2025.105432.
[13] X. Liu, X. Zhang, R. Ren, H.N. Mahmoud, Assessment of China's 20 years of infrastructure and policy development for flood disaster management, Int. J. Disaster Risk Reduct. 117 (2025) 105211, https://doi.org/10.1016/j.ijdrr.2025.105211.
[14] R.L. Knox, R.R. Morrison, E.E. Wohl, A river ran through it: floodplains as America's newest relict landform,, Sci. Adv. 8 (2022) eabo1082, https://doi.org/10.1126/sciadv.abo1082.
[15] W. Seher, L. Löschner, Balancing upstream–downstream interests in flood risk management: experiences from a catchment-based approach in Austria, J. Flood Risk Manag. 11 (2018) 56–65, https://doi.org/10.1111/jfr3.12266.
[16] N.V.K. Triet, N.V. Dung, H. Fujii, M. Kummu, B. Merz, H. Apel, Has dyke development in the Vietnamese Mekong Delta shifted flood hazard downstream? Hydrol. Earth Syst. Sci. 21 (2017) 3991–4010, https://doi.org/10.5194/hess-21-3991-2017.
[17] A.H. Ansari, A. Mejia, R. Cibin, Flood teleconnections from levees undermine disaster resilience, Npj Nat. Hazards 1 (2024) 1–9, https://doi.org/10.1038/s44304-024-00002-1.
[18] H.P. Jones, D.G. Hole, E.S. Zavaleta, Harnessing nature to help people adapt to climate change, Nat. Clim. Change 2 (2012) 504–509, https://doi.org/10.1038/nclimate1463.
[19] B.R. Forsberg, J.M. Melack, T. Dunne, R.B. Barthem, M. Goulding, R.C.D. Paiva, M.V. Sorribas, U.L.S. S Weisser Jr., The potential impact of new Andean dams on Amazon fluvial ecosystems, PLoS One 12 (2017) e0182254, https://doi.org/10.1371/journal.pone.0182254.
[20] F.E. Dunn, R.J. Nicholls, S.E. Darby, S. Cohen, C. Zarfl, B.M. Fekete, Projections of historical and 21st century fluvial sediment delivery to the Ganges-Brahmaputra-Meghna, Mahanadi, and Volta deltas, Sci. Total Environ. 642 (2018) 105–116, https://doi.org/10.1016/j.scitotenv.2018.06.006.
[21] C.L. McCabe, C.D. Matthaei, J.D. Tonkin, The ecological benefits of more room for Rivers,, Nat. Water 3 (2025) 260–270, https://doi.org/10.1038/s44221-025-00403-0.
[22] R.L. Knox, E.E. Wohl, R.R. Morrison, Levees don't protect, they disconnect: a critical review of how artificial levees impact floodplain functions, Sci. Total Environ. 837 (2022) 155773, https://doi.org/10.1016/j.scitotenv.2022.155773.
[23] C.N. Yuanita, S. Sagala, Blue-green infrastructure in Jakarta's fringe: an analysis of accessibility to blue-green spaces as a flood solution in Bekasi City, Int. J. Disaster Risk Reduct. (2025) 105425, https://doi.org/10.1016/j.ijdrr.2025.105425.
[24] K.-H. Liao, From flood control to flood adaptation: a case study on the lower green River Valley and the City of Kent in King County, Washington, Nat. Hazards 71 (2014) 723–750, https://doi.org/10.1007/s11069-013-0923-4.
[25] Q. Zhang, Z. Wu, P. Tarolli, Investigating the role of green infrastructure on urban WaterLogging: evidence from metropolitan coastal cities, Remote Sens. 13 (2021) 2341, https://doi.org/10.3390/rs13122341.

[26] C. Li, C. Peng, P.-C. Chiang, Y. Cai, X. Wang, Z. Yang, Mechanisms and applications of green infrastructure practices for stormwater control: a review, J. Hydrol 568 (2019) 626–637, https://doi.org/10.1016/j.jhydrol.2018.10.074.
[27] D. Green, E. O'Donnell, M. Johnson, L. Slater, C. Thorne, S. Zheng, R. Stirling, F.K.S. Chan, L. Li, R.J. Boothroyd, Green infrastructure: the future of urban flood risk management? Wires Water 8 (2021) e1560 https://doi.org/10.1002/wat2.1560.
[28] A.E. Bakhshipour, U. Dittmer, A. Haghighi, W. Nowak, Hybrid green-blue-gray decentralized urban drainage systems design, a simulation-optimization framework, J. Environ. Manag. 249 (2019) 109364, https://doi.org/10.1016/j.jenvman.2019.109364.
[29] X. Dong, H. Guo, S. Zeng, Enhancing future resilience in urban drainage system: green versus grey infrastructure, Water Res. 124 (2017) 280–289, https://doi.org/10.1016/j.watres.2017.07.038.
[30] Directorate-General for Environment (European Commission), Building a green infrastructure for Europe, Publ. Office Euro. Union (2014). https://data.europa.eu/doi/10.2779/54125. (Accessed 19 August 2025).
[31] M.G. Chung, K.A. Frank, Y. Pokhrel, T. Dietz, J. Liu, Natural infrastructure in sustaining global urban freshwater ecosystem services, Nat. Sustain. 4 (2021) 1068–1075, https://doi.org/10.1038/s41893-021-00786-4.
[32] UNESCO, Nature-Based Solutions for Water, Unesco, Paris, 2018.
[33] A. Staccione, A.H. Essenfelder, S. Bagli, J. Mysiak, Connected urban green spaces for pluvial flood risk reduction in the Metropolitan area of Milan, Sustain. Cities Soc. 104 (2024) 105288, https://doi.org/10.1016/j.scs.2024.105288.
[34] Y. Yao, J. Li, P. lv, N. Li, C. Jiang, Optimizing the layout of coupled grey-green stormwater infrastructure with multi-objective oriented decision making, J. Clean. Prod. 367 (2022) 133061, https://doi.org/10.1016/j.jclepro.2022.133061.
[35] I. Kowarik, L.K. Fischer, D. Haase, N. Kabisch, F. Kleinschroth, C. Konijnendijk, T.M. Straka, C. von Haaren, Promoting urban biodiversity for the benefit of people and nature, Nat. Rev. Biodivers. 1 (2025) 214–232, https://doi.org/10.1038/s44358-025-00035-y.
[36] M.A. Palmer, J. Liu, J.H. Matthews, M. Mumba, P. D'Odorico, Manage water in a green way, Science 349 (2015) 584–585, https://doi.org/10.1126/science.aac7778.
[37] C. Ye, W. Liao, Z. Xu, X. Li, X. Shu, An enhanced framework for simulating urban pluvial flooding: integrating nested watersheds and urban areas with spatial heterogeneity, J. Hydrol. 654 (2025) 132875, https://doi.org/10.1016/j.jhydrol.2025.132875.
[38] R. Morbidelli, C. Saltalippi, A. Flammini, C. Corradini, L. Brocca, R.S. Govindaraju, An investigation of the effects of spatial heterogeneity of initial soil moisture content on surface runoff simulation at a small watershed scale, J. Hydrol. 539 (2016) 589–598, https://doi.org/10.1016/j.jhydrol.2016.05.067.
[39] Y. Sun, J. Li, D. Yang, G. Bai, K. Guo, Impact of land use change on catchment stormwater flooding process based on a hydrodynamic model, J. Water Resourc. Water Eng. 31 (2020) 36, 40+46.
[40] K. Gabriels, P. Willems, J. Van orshoven, An iterative runoff propagation approach to identify priority locations for land cover change minimizing downstream river flood hazard, Landsc. Urban Plann. 218 (2022) 104262, https://doi.org/10.1016/j.landurbplan.2021.104262.
[41] I.-Y. Yeo, J.-M. Guldmann, Global spatial optimization with hydrological systems simulation: application to land-use allocation and peak runoff minimization, Hydrol. Earth Syst. Sci. 14 (2010) 325–338, https://doi.org/10.5194/hess-14-325-2010.
[42] P. Lu, N. Steffen, Y. Sun, Scenario-based performance assessment of green-grey-blue infrastructure for flood-resilient spatial solution: a case study of Pazhou, Guangzhou, greater Bay area, Landsc. Urban Plann. 238 (2023) 104804, https://doi.org/10.1016/j.landurbplan.2023.104804.
[43] Y. Xie, Restructuring cultural landscapes in metropolitan areas: characterization. Typology and Design Research, Springer Nature Singapore, Singapore, 2022, https://doi.org/10.1007/978-981-19-0755-5.
[44] Y. Xie, J. Ying, L. Chen, Typology, morphogenesis and adaptive transformation of polder landscape in the Yangtze River Delta, Urban Dev. Stud. 29 (2022) 70–77.
[45] C. Nolf, Y. Xie, F. Vannoorbeeck, B. Chen, Delta management in evolution: a comparative review of the Yangtze River Delta and rhine-meuse-scheldt Delta, Asia-Pac. J. Reg. Sci. 5 (2021) 597–624, https://doi.org/10.1007/s41685-020-00177-1.
[46] G. Zhang, Y. Wu, Irrigation dispute and government opration at the border between Jiangsu and Zhejiang: take provincial dispute caused by Wujiang County's joint polders in the 1950s-1960s as an example, Zhejiang Soc. Sci. (2012) 91, https://doi.org/10.14167/j.zjss.2012.09.003, 96+158.
[47] H. Zhang, S. Liu, Flood risk analysis and countermeasures for Taihu Lake and Taipu River, Yangtze River 51 (2020) 13–17, https://doi.org/10.16232/j.cnki.1001-4179.2020.02.003.
[48] P. Zhou, Y. Qi, Y. Song, L. Xie, B. Mao, Thought on water security governance in the Taihu Lake Basin under the challenge of climate change, Water Resour. Dev. Res. 23 (2023) 8–13, https://doi.org/10.13928/j.cnki.wrdr.2023.09.002.
[49] J. Wu, Z. Wu, H. Lin, H. Ji, M. Liu, Hydrological response to climate change and human activities: a case study of Taihu Basin, China,, Water Sci. Eng. 13 (2020) 83–94, https://doi.org/10.1016/j.wse.2020.06.006.
[50] H. Zhang, Q. Hong, Y. Jiang, Y. Xie, The synergistic effects of green-blue-gray infrastructure for flood risk management in plain river network areas, J. Environ. Manag. 392 (2025) 126671, https://doi.org/10.1016/j.jenvman.2025.126671.
[51] P. Lu, Y. Sun, Scenario-based hydrodynamic simulation of adaptive strategies for urban design to improve flood resilience: a case study of the Mingzhu Bay Region, Guangzhou, Greater Bay area,, River Res. Appl. 39 (2023) 1425–1436, https://doi.org/10.1002/rra.3913.
[52] V. Vema, K.P. Sudheer, I. Chaubey, Development of a hydrological model for simulation of runoff from catchments unbounded by ridge lines, J. Hydrol 551 (2017) 423–439, https://doi.org/10.1016/j.jhydrol.2017.06.012.
[53] C. Han, Q. Mei, S. Liu, G. Zhong, Research and application of hydrodynamic coupling model for plain tidal river network, J. Hydrodynam. Series A 29 (2014) 706–712.
[54] G. Zhong, S. Liu, Z. Hu, X. Zhang, Analysis of influence on region flood control due to polder waterlogging drainage in Yangcheng and Dianmao area, Yangtze River 48 (2017) 9–14, https://doi.org/10.16232/j.cnki.1001-4179.2017.21.002.
[55] C. Zhang, L. Wang, H. Zhu, H. Tang, Integrated hydrodynamic model for simulation of river-lake-sluice interactions, Appl. Math. Model. 83 (2020) 90–106, https://doi.org/10.1016/j.apm.2020.02.019.
[56] K.X. Soulis, Soil conservation service curve number (SCS-CN) method: current applications, remaining challenges, and future perspectives, Water 13 (2021) 192, https://doi.org/10.3390/w13020192.
[57] Y. Gao, M. Wu, Y. Liu, L. Gao, Z. Zhang, Analyzing the impact of polder-type flood control pattern on river system's regulation and storage capacity under urbanization, JAWRA J. Am. Water Resour. Assoc. 59 (2023) 1219–1245, https://doi.org/10.1111/1752-1688.13128.
[58] W. Luo, X. Wang, W. Qiao, J. Sun, L. Qian, H. Fu, Effects of land use change on drainage modulus in plain lake area based on a coupled hydrological and hydrodynamic model, J. Yangtze River Sci. Res. Inst. 35 (2018) 76, https://doi.org/10.11988/ckyyb.20161226.
[59] R. Drobot, A. Draghia, Coupled hydrological and hydraulic modeling for flood mapping, EGU General Assembly (2014).
[60] M. Zhang, D. Peng, H. Lin, L. Qiu, The impact of land use changes on streamflow in Taihu basin, J. Beijing Normal Univ. (Nat. Sci.) 50 (2014) 467–471.
[61] W. Cheng, C. Wang, Y. Zhu, Taihu Basin Model, Hohai University Press, 2006.
[62] H. Zhao, L. Zhou, R. Zhao, Z. Li, Z. Qi, Flood Process Modeling in the Plain Basin Based on MIKE Coupling Model, China Rural Water and Hydropower, 2022, pp. 97–102.
[63] S. Zhou, Z. Liu, M. Wang, W. Gan, Z. Zhao, Z. Wu, Impacts of building configurations on urban stormwater management at a block scale using XGBoost, Sustain. Cities Soc. 87 (2022) 104235, https://doi.org/10.1016/j.scs.2022.104235.
[64] J.J. Opperman, G.E. Galloway, Nature-based solutions for managing rising flood risk and delivering multiple benefits, One Earth 5 (2022) 461–465, https://doi.org/10.1016/j.oneear.2022.04.012.
[65] E. Penning, R.P. Burgos, M. Mens, R. Dahm, K. de Bruijn, Nature-based solutions for floods AND droughts AND biodiversity: do we have sufficient proof of their functioning? Cambridge Prisms: Water 1 (2023) e11, https://doi.org/10.1017/wat.2023.12.
[66] J. Aerts, M. Van Herwijnen, R. Janssen, T. Stewart, Evaluating spatial design techniques for solving land-use allocation problems, J. Environ. Plann. Manag. 48 (2005) 121–142, https://doi.org/10.1080/0964056042000308184.

[67] X. Li, X. Ma, An improved simulated annealing algorithm for interactive multi-objective land resource spatial allocation, Ecol. Complex. 36 (2018) 184–195, https://doi.org/10.1016/j.ecocom.2018.08.008.
[68] C. Spearman, The proof and measurement of association between two things, Am. J. Psychol. 15 (1904) 72–101, https://doi.org/10.2307/1412159.
[69] W.S. Cleveland, Robust locally weighted regression and smoothing scatterplots, J. Am. Stat. Assoc. 74 (1979) 829–836, https://doi.org/10.1080/01621459.1979.10481038.
[70] E. Rafiei-Sardooi, A. Azareh, B. Choubin, A.H. Mosavi, J.J. Clague, Evaluating urban flood risk using hybrid method of TOPSIS and machine learning, Int. J. Disaster Risk Reduct. 66 (2021) 102614, https://doi.org/10.1016/j.ijdrr.2021.102614.
[71] J. Wu, J. Xu, M. Lu, H. Ming, An integrated modelling framework for optimization of the placement of grey-green-blue infrastructure to mitigate and adapt flood risk: an application to the Upper Ting River Watershed, China, J. Hydrol.: Reg. Stud. 57 (2025) 102156, https://doi.org/10.1016/j.ejrh.2024.102156.
[72] K. Gunnell, M. Mulligan, R.A. Francis, D.G. Hole, Evaluating natural infrastructure for flood management within the watersheds of selected global cities, Sci. Total Environ. 670 (2019) 411–424, https://doi.org/10.1016/j.scitotenv.2019.03.212.
[73] B. Barnhart, P. Pettus, J. Halama, R. McKane, P. Mayer, K. Djang, A. Brookes, L.M. Moskal, Modeling the hydrologic effects of watershed-scale green roof implementation in the Pacific Northwest, United States, J. Environ. Manag. 277 (2021) 111418, https://doi.org/10.1016/j.jenvman.2020.111418.
[74] A. Shaamala, T. Yigitcanlar, A. Nili, D. Nyandega, Algorithmic green infrastructure optimisation: review of artificial intelligence driven approaches for tackling climate change, Sustain. Cities Soc. 101 (2024) 105182, https://doi.org/10.1016/j.scs.2024.105182.
[75] F. Naseri, M. Azari, M.T. Dastorani, Spatial optimization of soil and water conservation practices using coupled SWAT model and evolutionary algorithm, Int. Soil Water Conserv. Res. 9 (2021) 566–577, https://doi.org/10.1016/j.iswcr.2021.04.002.
[76] M. Barah, A. Khojandi, X. Li, J. Hathaway, O. Omitaomu, Optimizing green infrastructure placement under precipitation uncertainty, Omega 100 (2021) 102196, https://doi.org/10.1016/j.omega.2020.102196.
[77] S. Haghighatafshar, B. Nordlöf, M. Roldin, L.-G. Gustafsson, J. La Cour Jansen, K. Jönsson, Efficiency of blue-green stormwater retrofits for flood mitigation – conclusions drawn from a case study in Malmö, Sweden, J. Environ. Manag. 207 (2018) 60–69, https://doi.org/10.1016/j.jenvman.2017.11.018.
[78] T. Xu, B.A. Engel, X. Shi, L. Leng, H. Jia, S.L. Yu, Y. Liu, Marginal-cost-based greedy strategy (MCGS): fast and reliable optimization of low impact development (LID) layout, Sci. Total Environ. (2018).
[79] L. Torres-Rojas, N. Vergopolan, J.D. Herman, N.W. Chaney, Towards an optimal representation of sub-grid heterogeneity in land surface models, Water Resour. Res. 58 (2022) e2022WR032233, https://doi.org/10.1029/2022WR032233.
[80] S. Kato, W. Huang, Land use management recommendations for reducing the risk of downstream flooding based on a land use change analysis and the concept of ecosystem-based disaster risk reduction, J. Environ. Manag. 287 (2021) 112341, https://doi.org/10.1016/j.jenvman.2021.112341.
[81] Q. Wang, J. Chen, Spatio-temporal evaluation of the emergency capacity of the cross-regional rain-flood disaster in the Yangtze River Economic Belt in China, Sci. Rep. 11 (2021) 2580, https://doi.org/10.1038/s41598-021-82347-5.
[82] J. Best, Anthropogenic stresses on the world's big rivers, Nat. Geosci. 12 (2019) 7–21, https://doi.org/10.1038/s41561-018-0262-x.
[83] Mathilde de Go er de Herve, Fair strategies to tackle unfair risks? Justice considerations within flood risk management, Int. J. Disaster Risk Reduct. 69 (2022) 102745, https://doi.org/10.1016/j.ijdrr.2021.102745.
[84] T. Thaler, L. Löschner, T. Hartmann, The introduction of catchment-wide co-operations: scalar reconstructions and transformation in Austria in flood risk management,, Land Use Policy 68 (2017) 563–573, https://doi.org/10.1016/j.landusepol.2017.08.023.
[85] A.S. Mehta, J.F. Warner, Multi-level hegemony in transboundary flood risk management: a downstream perspective on the maritsa Basin,, Environ. Sci. Pol. 129 (2022) 126–136, https://doi.org/10.1016/j.envsci.2021.12.014.
[86] J.J. Rouillard, T. Ball, K.V. Heal, A.D. Reeves, Policy implementation of catchment-scale flood risk management: learning from Scotland and England, Environ. Sci. Pol. 50 (2015) 155–165, https://doi.org/10.1016/j.envsci.2015.02.009.
[87] T. Thaler, R. Nordbeck, L. Löschner, W. Seher, Cooperation in flood risk management: understanding the role of strategic planning in two Austrian policy instruments, Environ. Sci. Pol. 114 (2020) 170–177, https://doi.org/10.1016/j.envsci.2020.08.001.
[88] R.A.S. Machado, A.G. Oliveira, R.C. Lois-González, Urban ecological infrastructure: The importance of vegetation cover in the control of floods and landslides in Salvador / Bahia, Brazil, Land Use Policy 89 (2019) 104180, https://doi.org/10.1016/j.landusepol.2019.104180.
[89] J. Kerr, Watershed development, environmental services, and poverty alleviation in India, World Dev. 30 (2002) 1387–1400, https://doi.org/10.1016/S0305-750X(02)00042-6.
[90] T. Thaler, T. Hartmann, Justice and flood risk management: reflecting on different approaches to distribute and allocate flood risk management in Europe, Nat. Hazards 83 (2016) 129–147, https://doi.org/10.1007/s11069-016-2305-1.
[91] S. Pauleit, B. Ambrose-Oji, E. Andersson, B. Anton, A. Buijs, D. Haase, B. Elands, R. Hansen, I. Kowarik, J. Kronenberg, T. Mattijssen, A. Stahl Olafsson, E. Rall, A. P.N. van der Jagt, C. Konijnendijk van den Bosch, Advancing urban green infrastructure in Europe: outcomes and reflections from the GREEN SURGE project, Urban For. Urban Green. 40 (2019) 4–16, https://doi.org/10.1016/j.ufug.2018.10.006.
[92] L. Peskett, M.J. Metzger, K. Blackstock, Regional scale integrated land use planning to meet multiple objectives: good in theory but challenging in practice, Environ. Sci. Pol. 147 (2023) 292–304, https://doi.org/10.1016/j.envsci.2023.06.022.
[93] Y. Xie, J. Zou, Y. Chen, F. Li, Q. Jiang, Are wading birds the ideal focal species for broader bird conservation? A cost-effective approach to ecological network planning, Ecol. Indic. 160 (2024) 111785, https://doi.org/10.1016/j.ecolind.2024.111785.
[94] D. Zhen, D. Liu, X. Zhao, H. Liu, H. Zhu, Innovation of trans-boundary collaborative regional integration planning: green zones and integrated ecological development of the Yangtze River Delta, Urban Planning Forum (2022) 3–8, https://doi.org/10.16361/j.upf.202208001.
[95] GWP, Integrated Water Resources Management, Global water partnership, Stockholm, 2000.
[96] M. Ben-Daoud, B.E. Mahrad, I. Elhassnaoui, A. Moumen, A. Sayad, M. Elbouhadioui, G.A. Moroşanu, L.E. Mezouary, A. Essahlaoui, S. Eljaafari, Integrated water resources management: an indicator framework for water management system assessment in the R'Dom Sub-basin, Morocco, Environ. Chall. 3 (2021) 100062, https://doi.org/10.1016/j.envc.2021.100062.
[97] J.Y. Al-Jawad, H.M. Alsaffar, D. Bertram, R.M. Kalin, A comprehensive optimum integrated water resources management approach for multidisciplinary water resources management problems, J. Environ. Manag. 239 (2019) 211–224, https://doi.org/10.1016/j.jenvman.2019.03.045.
[98] J. Wang, J. Liu, Z. Yang, C. Mei, H. Wang, D. Zhang, Green infrastructure optimization considering spatial functional zoning in urban stormwater management, J. Environ. Manag. 344 (2023) 118407, https://doi.org/10.1016/j.jenvman.2023.118407.